IVYSPRING INTERNATIONAL PUBLISHER

Theranostics

2017; 7(16): 3876-3888. doi: 10.7150/thno.19547

Research Paper

# Multimodal Assessment of Mesenchymal Stem Cell Therapy for Diabetic Vascular Complications

Jamila Hedhli[1, 2], Christian J. Konopka[1, 2], Sarah Schuh[2], Hannah Bouvin[1], John A. Cole[3], Heather D. Huntsman[1, 4], Kristopher A. Kilian[2], Iwona T. Dobrucki[1], Marni D. Boppart[1, 4], Lawrence W. Dobrucki[1, 2]✉

1. Beckman Institute for Advanced Science and Technology, Urbana, IL;
2. Department of Bioengineering, University of Illinois at Urbana-Champaign, Urbana, IL;
3. Department of Physics, University of Illinois at Urbana-Champaign, Urbana, IL;
4. Department of Kinesiology, University of Illinois at Urbana-Champaign, Urbana, IL.

✉ Corresponding author: Lawrence W. Dobrucki, Email: dobrucki@illinois.edu 405 N. Mathews Ave, MC-251, Urbana, IL 61801



Received: 2017.02.07; Accepted: 2017.06.07; Published: 2017.09.05

## Abstract

Peripheral arterial disease (PAD) is a debilitating complication of diabetes mellitus (DM) that leads to thousands of injuries, amputations, and deaths each year. The use of mesenchymal stem cells (MSCs) as a regenerative therapy holds the promise of regrowing injured vasculature, helping DM patients live healthier and longer lives. We report the use of muscle-derived MSCs to treat surgically-induced hindlimb ischemia in a mouse model of type 1 diabetes (DM-1). We serially evaluate several facets of the recovery process, including $\alpha_V\beta_3$-integrin expression (a marker of angiogenesis), blood perfusion, and muscle function. We also perform microarray transcriptomics experiments to characterize the gene expression states of the MSC-treated is- chemic tissues, and compare the results with those of non-ischemic tissues, as well as ischemic tissues from a saline-treated control group.

The results show a multifaceted impact of mMSCs on hindlimb ischemia. We determined that the angiogenic activity one week after mMSC treatment was enhanced by approximately 80% relative to the saline group, which resulted in relative increases in blood perfusion and muscle strength of approximately 42% and 1.7-fold, respectively. At the transcriptomics level, we found that several classes of genes were affected by mMSC treatment. The mMSCs appeared to enhance both pro-angiogenic and metabolic genes, while suppressing anti-angiogenic genes and certain genes involved in the inflammatory response. All told, mMSC treatment appears to exert far-reaching effects on the microenvironment of ischemic tissue, enabling faster and more complete recovery from vascular occlusion.

Key words: Angiogenesis, PET-CT, Dimeric-cRGD, Multimodal imaging, Peripheral arterial disease (PAD), Diabetes, Muscle-derived mesenchymal stem cells (mMSCs).

## Introduction

Diabetes represents a major world-wide health concern. Hung *et al.* projects that between 2009 and 2034 the number of people with diabetes will increase from 23.7 million to 44.1 million, resulting in a significant strain to the global health care system with a projected increase in relative cost of almost 4-fold [1]. The Centers for Disease Control (CDC) in a 2014 diabetes report card estimated that about 1.7 million new cases of diabetes are diagnosed each year, and predicted a sharp rise in the next couple of years, during which an estimated of 1 in 3 adults will be diagnosed [2].

Cardiovascular complications are among the leading causes of morbidity and mortality in diabetic patients, and account for over 80% of diabetes-associated deaths. One of the most serious is peripheral arterial disease (PAD), which is characterized as a narrowing of the peripheral

vasculature. Very often patients with PAD can be asymptomatic, making the condition difficult to recognize and treat. As a result, the blood flow to patients' extremities can become progressively impaired, and ischemia can occur. When ineffectively treated, peripheral ischemia can result in debilitating injury; in the United States alone roughly 50,000 cases each year lead to amputation [1]. The main cause of the poor clinical outcome of diabetes mellitus (DM) patients suffering from PAD is their reduced capacity for neovascularization, an important bodily response to vascular occlusion [3]. Despite considerable technological advancement, mortality and both morbidity resulting from PAD remain high, even before diagnosis or treatment thresholds are met.

Lifestyle changes and increased exercise are regarded as the most effective treatment for complications associated with PAD. In more critical PAD cases, therapies generally rely on mechanical revascularization through either percutaneous or surgical approaches. Unfortunately, these approaches are frequently unsuccessful in the long term. More recently, novel therapies involving the delivery of proangiogenic factors, either directly or through gene transfer, have been introduced, with some now in clinical trials [4–6]. The majority of these new therapies target only a single biomarker associated with PAD, such as vascular endothelial (VEGF) or fibroblast growth factors (FGF). Due to the complexities of the biochemical networks involved, however, such oversimplified approaches often fail to give rise to demonstrable improvements in actual patients. More holistic interventions capable of altering the microenvironment of endothelial cells and rendering them suitable for angiogenesis could be more effective. As a result, interest has shifted toward cell-based approaches utilizing the potential of progenitor and stem cells as agents of tissue repair and neovascularization.

Targeted stem cell-based therapies appear to provide clinical improvement for PAD patients by enhancing vascular density (angiogenesis), initiating large vessel remodeling (arteriogenesis), and ultimately improving blood perfusion [7]. Of the various potential candidate cells that might be used in treating PAD patients, mesenchymal stem cells (MSCs) are being pursued the most actively at both preclinical and clinical levels [7]. Several properties of MSCs make them well suited to the task. Most importantly, through their paracrine-related effects, MSCs have been shown to promote angiogenesis, arteriogenesis, and terminally differentiate into vascular cells and myocytes [8]. They have also been shown to release anti-apoptotic, anti-fibrotic, immunomodulating, and chemoattractant factors, and their inherent metabolic flexibility and resistance to ischemic stress has been shown to facilitate their survival in ischemic environments [9]. Muscle-derived MSCs (mMSCs) are particularly attractive due to their abundance and the ease with which they can be extracted. The surgical excisement of skeletal muscle tissue carries little risk, and the subsequent isolation and culturing of mMSCs is extremely straightforward. Moreover, their long-term passaging capacity and immunomodulatory properties could allow for allogeneic transplantation into many different tissues with little risk of rejection.

Previous studies involving diabetic mice have shown that angiogenesis is directly impaired by the high endothelial glucose levels associated with diabetes [10]. As a result, the long-term effects of uncontrolled diabetic hyperglycemia include ischemia, especially in the extremities, and subsequent debilitating injury. In this article, we investigate the use of mMSCs to treat surgically-induced hindlimb ischemia in a diabetic mouse model of PAD. We employ several minimally invasive *in vivo* imaging and diagnostic approaches (nuclear, laser Doppler perfusion, muscle function and microarray transcriptomics) in order to construct an accurate picture of the effects of our transplanted mMSCs, as well as the response of our mice to treatment, and their long-term prognosis. We find that mMSCs lead to greatly enhanced neovascularization roughly one week after treatment. We also find that at the two-week time point, the transcriptional profile of our stem-cell treated mice resembles that of healthy mice while a control group treated with saline continue to express anti-angiogenic factors, indicating a relative lack of healing. The translational nature and timeliness of this work is significant, and our results have potentially important clinical implications for the evaluation and management of diabetic patients with PAD. Also, noteworthy is the impressive specificity and favorable biodistribution of the molecular probe used in our nuclear imaging studies. The clinical implications of using targeted molecular imaging in PAD are substantial, as they can help to detect diseases earlier, evaluate treatment effectiveness over time, and ultimately help to tailor therapy regimens to individual patients.

## Materials and Methods

Our research plan is outlined in Figure 1. Briefly, type 1 diabetes was chemically induced in 4 to 6-week old mice; their right femoral arteries were ligated to mimic PAD, and they were treated with either sterile saline (control) or transplanted with mMSCs isolated from a different group of animals of similar age and genotype. After treatment, the ischemic DM animals

were assessed for angiogenesis (PET-CT), blood perfusion (LDF), and muscle function (FUNC) at different time points after surgery.

### Isolation of muscle-derived mesenchymal stem cells (mMSCs) from skeletal muscle

Five-week old C57BL/6 mice gastrocnemius-soleus complexes were excised, mechanically and enzymatically digested, filtered, and incubated with anti-mouse CD16/CD32 (Ebioscience, USA) in order to block non-specific Fc-mediated interactions. Cells were then stained with both monoclonal anti-mouse Sca-1$^+$PE (Ebioscience, USA) and CD45$^-$APC (Ebioscience, USA) antibodies and isolated with FACS. Sca-1$^+$CD45$^-$ cells were then collected in media for culture.

### Cell Culture

mMSCs were grown to confluence in Dulbecco's Modification of Eagle's medium (DMEM, Fisher Scientific, USA), containing 10% heat-inactivated FBS (Invitrogen), 100 U/mL penicillin G, and 100 $\mu$g/mL gentamicin, and were maintained in a humidified incubator at 37°C with 5% $CO_2$.

### Western blotting

mMSCs and human umbilical vein endothelial cells (HUVEC, known to express $a_V\beta_3$) were washed three times in sterile phosphate-buffered saline (PBS). Cell pellets were collected by centrifugation and incubated in a solution of RIPA buffer (Sigma-Aldrich, USA) and Protease Inhibitor (Sigma-Aldrich, USA). The cocktail was sonicated 3 times for a length of 20 seconds with a 10 second incubation on ice. The lysed cells were centrifuged for 15 min and the supernatant (protein) was collected. The concentration of protein was determined using Gen5 Microplate Reader and Imager Software (BioTek Instruments, USA). A total of 20-10 ng of proteins were resolved on 10% SDS-polyacrylamide gel electrophoresis and transferred onto PVDF membranes (Immobilon, Millipore). Membranes were blocked in Tris-buffered saline (TBS) containing 10% non-fat dry milk and 0.1% Tween 20, prior to incubation with 80 $\mu$Ci of $^{64}$Cu-NOTA-PEG$_4$-cRGD$_2$ targeted to $a_V\beta_3$ (a well characterized marker of angiogenesis) for 1 hour at room temperature. After washing the membrane with PBS, they were transferred on the multisensitive phosphor screen (Perkin-Elmer, USA) and imaged with Cyclone Plus Storage Phosphor System (Perkin-Elmer, USA).

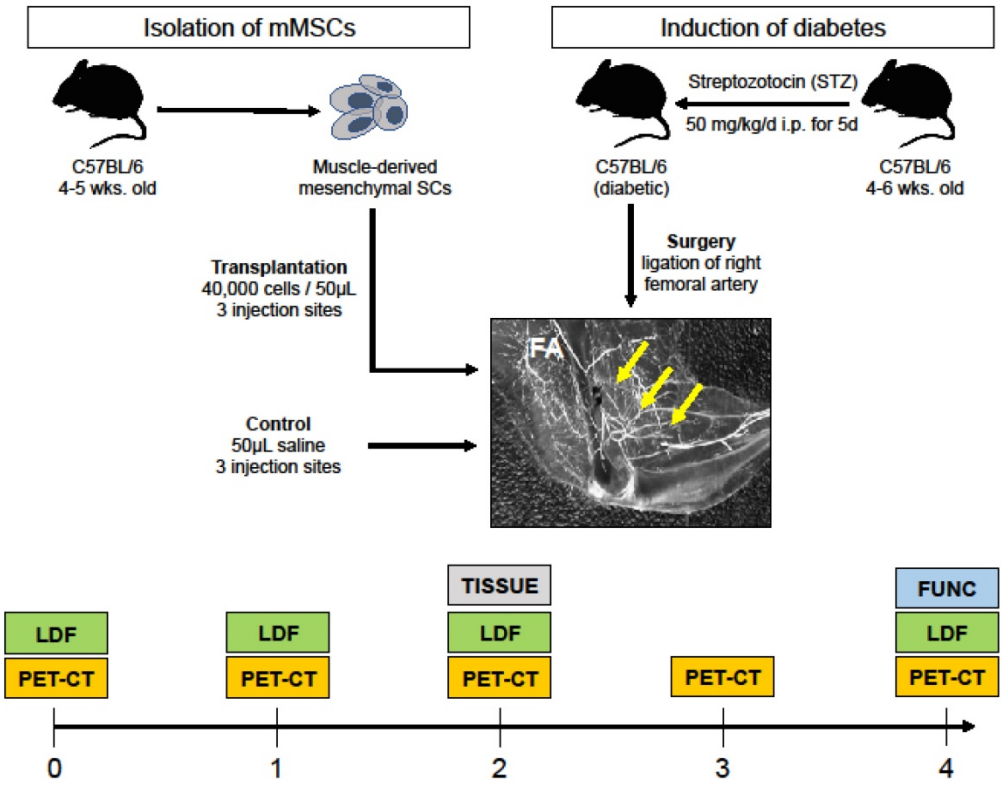


**Figure 1.** Study overview. Streptozotocin was used to induce DM in 4 to 6 week old C57BL/6 mice. The right femoral artery of the DM mice was then ligated to mimic PAD. mMSCs were isolated from another group of mice and then injected into three different sites in the ischemic gastrocnemius-soleus of DM group. A control group received saline injections. Both experimental and control groups were serially evaluated for $\alpha_V\beta_3$ expression (using PET-CT), blood perfusion (using laser Doppler flow, LDF), and muscle function (denoted FUNC). At week two, skeletal muscle tissue was extracted for immunohistochemistry and microarray transcriptomics experiments (denoted TISSUE).

## Angiogenic cytokines array

For cytokine analysis of protein extracted from ischemic tissue of stem cell and saline animals, we used mouse antibody angiogenesis array membrane (Abcam ab139697, 24 target proteins) as per manufacturer instructions. Protein samples were incubated with blocked membranes overnight with the membranes at 4°C. Prepared membranes were exposed for the protein detection. The membranes were scanned and analyzed using Biorad Image Lab 5.2 software. The signal was normalized to the positive control signal intensity as proposed by the manufacturer.

## *In vivo* evaluation

### Animal preparation

All *in vivo* imaging experiments were performed with the approval of the Institutional Animal Care and Use Committee of the University of Illinois at Urbana-Champaign, following the principles outlined by the American Physiological Society on research animal use.

### Permanent hindlimb ischemia in DM mice

Type-1 DM was induced by streptozotocin (STZ) administration (50 mg/kg, i.p. daily for 5 consecutive days) in two months old male wild-type mice (C57BL/6). Previous studies have documented that STZ induces moderate diabetes in 85% male mice with survival up to 4 months after treatment without receiving insulin administration. Mice with fasting glycemia (>200 mg/dL) at 14 days after the first STZ treatment were considered diabetic. Mice were anesthetized with isoflurane and unilateral hindlimb ischemia was surgically induced by femoral artery ligation following previously published approaches [11]. Animals were matched for age and sex, and divided into two groups: a control group (n=10) which was subjected to saline i.m. injections, and an experimental group (n=10) that recieved mMSC i.m. injections. Before the ligation, and at 1, 2, 3 and 4 weeks after the ligation, all animals were delivered to our microPET/SPECT/CT facility for molecular imaging, assessment of perfusion and muscular function.

### mMSCs transplantation into hindlimb muscle

Cultured muscle-derived Sca-1$^{+}$CD45$^{-}$ cells were collected and suspended in Hanks Balanced Saline Solution (HBSS). Immediately after ligation of the femoral artery (see Section 2.5), the experimental group received intramuscular injections of ~ $4 \times 10^4$ cells in 50 $\mu$L of sterile HBSS into three sites in the gastrocnemius muscle of right hindlimb, while the control group recieved injections of sterile HBSS only. Our group has established the optimal number of cells for injection from a previously [9].

### *In vivo* molecular imaging of angiogenesis and perfusion

One week prior to surgical induction of hindlimb ischemia, as well as 1, 2, 3, and 4 weeks after, all animals were anesthetized with 1-3% isoflurane, the neck area was shaved, and the left jugular vein was isolated for placement of a PE-10 polyurethane catheter (Fisher Scientific, USA) to facilitate administration of the radiotracer. The animals were injected with ~30 MBq of $^{64}$Cu-NOTA-PEG$_4$-cRGD$_2$ targeted at $a_V\beta_3$, a well characterized marker of angiogenesis [12]. Imaging was performed using a dedicated small animal microPET-CT scanner (Inveon, Siemens Healthcare, USA). The animals were placed on the animal bed and ~60 min after radiotracer injection, a 15 min microPET imaging session was performed. PET imaging was followed by a high-resolution anatomical microCT imaging (360 projections, 80 keV/500 $\mu$A energy).

The microPET and microCT images were reconstructed using OSEM/3D algorithm (Siemens Healthcare USA) and cone-beam technique (Cobra Exim), respectively. MicroPET were fused with microCT images and quantified using semi-automated approach developed and evaluated by our group previously [11]. Briefly, complex irregular volumes of interest (VOIs) were generated from the microCT images and applied on the co-registered microPET images to calculate absolute $^{64}$Cu activities using Inveon Research Workplace (Siemens Healthcare USA). These complex VOIs included only soft tissue (skeletal muscles) after the removal of bone structures during the image segmentation process.

At the same time points (one week prior, and 1, 2, and 4 weeks after surgery) all animals were measured with a needle-like laser Doppler probe (BioPac systems, USA) to assess peripheral perfusion as described in [13]. Succinctly after the probe was calibrated to a known motility standard, the needle was inserted into the gastrocnemius muscle to output a signal that was proportional to the red blood cell perfusion in that area and expressed in blood perfusion units. Peripheral perfusion was reported as a ratio of ischemic to non-ischemic limb of the same animal.

### Measurement of the muscular function

To assess the muscular recovery of the animals, an invasive contractile force measurement technique was employed. After the final imaging session at four weeks after surgery animal's maximal isometric

hindlimb plantar flexor force was measured using a dual-lever system described previously [14]. Briefly, under anesthesia the animal's sciatic nerve was electrically stimulated, and the resulting muscle forces were measured with a servomotor and control unit (Aurora Scientific, USA). Stimulation was repeated 9 times with 5 s recovery periods for a total of 10 measurements. For each animal, the value of the maximal force output (g) was normalized to the muscle mass (g), and expressed as a ratio of ischemic to non-ischemic limb of the same animal.

### Statistical analysis

The Student t test was used to compare 2 groups. One-way ANOVA was used to compare multiple parameters. A value of $P < 0.05$ was considered significant.

## Post mortem Analysis

### Biodistribution

For biodistribution studies, all animals were euthanized at 90 min post-injection and selected organ samples were collected for gamma well counting analysis. All collected sections were weighed and the tissue radioactivity was measured with Wizard$^2$ gamma well counter (Perkin-Elmer, USA). Measured $^{64}$Cu activity was corrected for background, decay time, and tissue weight, and expressed as percent of injected dose per tissue weight (%I.D./g).

### Histology and immunohistofluorescence

A subset of the animals was euthanized at 2 weeks post-surgery and their gastrocnemius/soleus muscle complexes were excised, embedded in TissueTec (Sakura, USA) and snap frozen in -150˚C methylbutane. Frozen sections (5 nm) were placed on microscope slides, fixed with pre-cooled acetone, and stored at -80˚C before staining. To assess skeletal muscle vascularity, muscle samples were stained with an endothelial cell- specific marker PE anti-mouse CD31 Antibody (Abcam, USA). All staining procedures were performed according to the product-specific protocols (four for each slide). The stains were quantified for extent (percentage area) of positive staining in randomly chosen high-powered (200 ×) fields using algorithms validated by our group previously [15].

## Transcriptomics

### RNA extraction protocol

Total gastrocnemius/soleus muscle RNAs (ligated and non-ligated) from the saline and mMSCs treated mice were isolated using an RNeasy tissue mini-kit (QIA- GEN). RNA quality was measured using an Agilent Bioanalyzer and quantified using a Qubit Fluorometer (Life Technologies) before microarray analysis.

### Hybridization protocol

Saline- or mMSCs- treated skeletal muscle (n = 4 each) were paired with a non-ischemic sample on an array; samples came from the same mouse. We employed a dye-balance design such that of the four replicates of each treated group, two were in red (Cy5) and two were in green (Cy3). A total RNA of 200 ng was labeled using the Agilent 2-color Low Input Quickamp Labeling kit (Agilent Technologies, Santa Clara, CA) according to the manufacturer's protocols. Labeled samples were hybridized to an Agilent mouse 4x44K array and scanned on an Axon 4000B microarray scanner (Molecular Devices, Sunnyvale, CA) at 5 $\mu$m resolution. Spotfinding was carried out using GenePix 6.1 image analysis software (Molecular Devices, Sunnyvale,CA).

### Microarray analysis description

Microarray data pre-processing and statistical analyses were done in R (v 3.3.2) [16] using the limma package (v3.30.6) [17]. Median foreground and median background values from the eight arrays were read into R; no spots were manually flagged as bad. The background was low and even across the arrays, and as such, it was ignored. M-values ($ln(2)(Cy5/Cy3)$) for each array were normalized first with the traditional loess within-array normalization, and then the scale between-array normalization [18]. Agilent's Mouse Gene Expression v2 4x44K Microarray interrogates 23,254 genes using 39,030 probes spotted one time (1X), and 399 probes spotted ten times (10X) each based on current annotation information. Correlations between the replicate spots for each probe were high, and so the M-values for replicate spots were simply averaged for each sample. The positive and negative control probes were used to assess what minimum expression level could be considered "detectable above background noise" (5.75 on the ln (2) scale) and then the control probes were discarded. Further quality control investigations were done on individual Cy5 and Cy3 values that were quantile normalized to assess variation among individual samples [18]. Because of the high correlations associated with the mouse/array pairings, and no observable difference between the non-ischemic samples, all statistical analyses were done on the M-values rather than the single-channel values. This is preferable because the M-values implicitly control for mouse/array pairings using limmas empirical Bayes model that includes a term for the dyes [19]. The

equivalent of a one-way ANOVA test was pulled from the model to detect any differences across the three groups (non-ischemic, ischemic saline-treated, and ischemic mMSC-treated). These ANOVA values were used along with updated mappings of probes to Entrez Gene IDs from Bioconductors MmAgilentDesign026655.db (v 3.4.0) [20] to reduce the 39,429 unique probes down to a set of 11,885 representing expressed, unique genes: first, probes without quantile-normalized expression values > 5.75 in at least 3 of the 16 samples (21,752 probes) were removed; second, probes that did not map to any Entrez Gene ID (2,712 probes) were removed; and lastly for the 2,566 genes with more than one remaining probe, a single probe based on the lowest ANOVA raw p-value was selected. Prior to the statistical analysis, a literature search resulted in 149 genes known to be involved with angiogenesis or peripheral arterial disease. An additional 234 genes (for a total of 383) were identified by finding genes annotated to any of the 26 Gene Ontology terms with angiogenesis in the name based on Bioconductors org.Mm.eg.db package (v 3.4.0). In addition to a one-way ANOVA, three pairwise comparisons were also pulled from the model: saline vs. control, stem cell vs. control and stem cell vs. saline. The False Discovery Rate (FDR) correction was performed separately for the 383 a priori gene set and for the 11,522 additional genes detected above background by the microarray, as well as globally for the one-way ANOVA + 3 pairwise comparisons. Heat maps for specific genes were made from the quantile-normalized separate channel values, after removing array and dye effects, then scaling each gene to have a mean of zero and a standard deviation of one.

## Results

### mMSCs enhance angiogenic activity, perfusion, and muscle function in DM mice

To non-invasively assess the angiogenic activity of mMSC-treated DM mice, we injected and imaged our $\alpha_V\beta_3$-targeted PET-CT probe, $^{64}$Cu-NOTA-PEG$_4$-cRGD$_2$, at a series of time- points after the onset of hindlimb ischemia (see Figure 2). During image analysis, we determined the mean signal within volumes of interest corresponding to both the ischemic and non-ischemic legs of each animal. Their ratio (mean ischemic to non-ischemic) represents a measure of each animal's response to mMSC (or saline) treatment. We determined that angiogenic activity one week after mMSC treatment was enhanced by approximately 80% relative to the saline control group (see Figure 3A). This enhancement carried forward to week two in which we found a 40% relative increase. Weeks 3 and 4 were comparable in both groups.

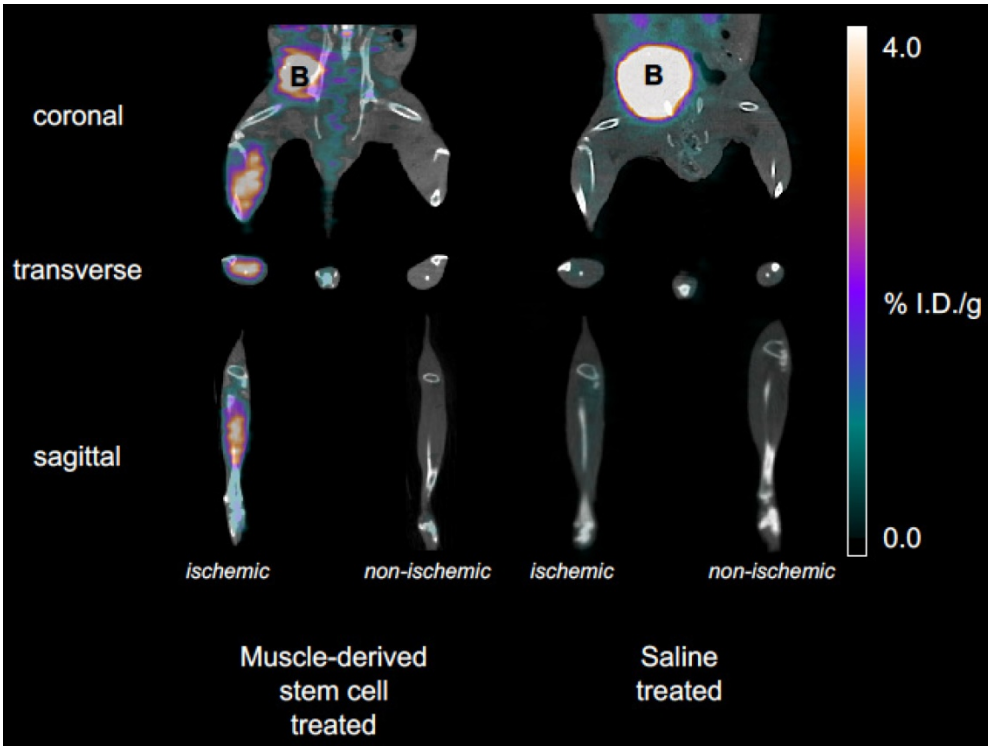


**Figure 2.** Representative PET-CT images. Coronal, transverse, and sagittal views are shown for both mMSC- and saline-treated mice at 1 week post-surgery and implantation. The mMSC-treated mice show significant $\alpha v\beta_3$-targeted probe accumulation in the ischemiclimb.

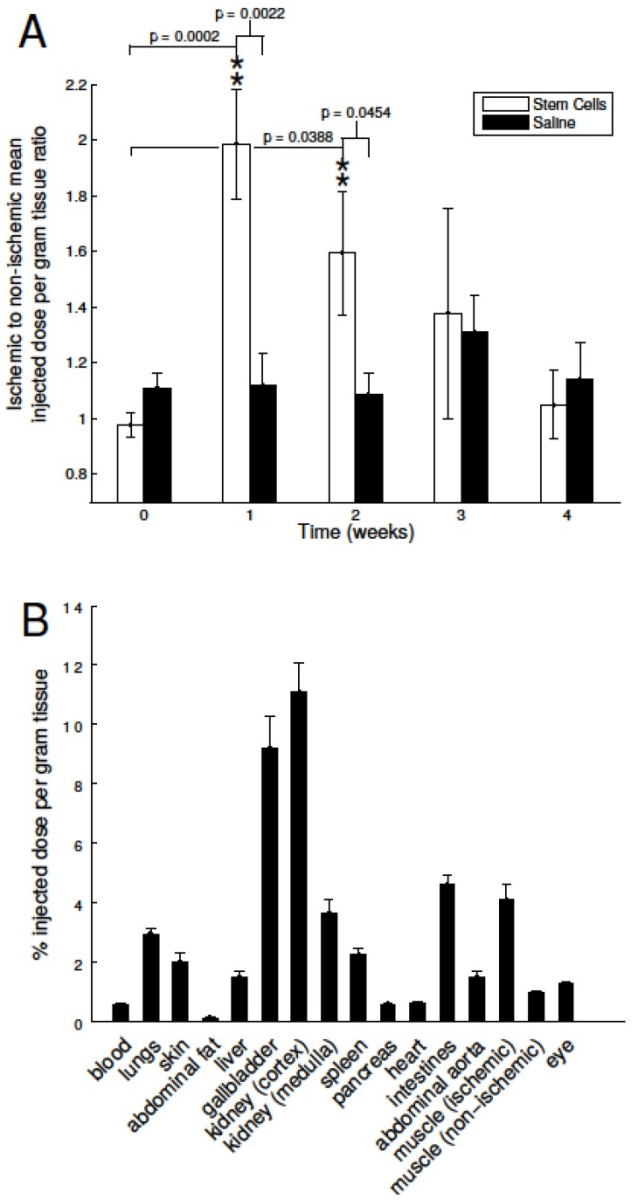


**Figure 3.** Image based analysis of $\alpha v\beta_3$ expression and biodistribution. A) $^{64}$Cu-NOTA-PEG$_4$-cRGD$_2$ was used to noninvasively assess $\alpha v\beta_3$ expression before femoral artery ligation (week zero, baseline) and one, two, three, and four weeks after. mMSC-treated mice showed significant enhancement relative to both the baseline and the saline- treated group at the one and two week time points. B) The biodistribution assessed with gamma well counting of radiolabeled $^{64}$Cu-NOTA-PEG$_4$-cRGD$_2$ targeted at $\alpha v\beta_3$ integrin demonstrated a favorable biodistribution and optimal retention for targeted *in vivo* imaging of peripheral angiogenesis in n=4 animals treated with mMSCs.

Neovascularization is the first stage of angiogenic recovery. We investigated whether enhanced $a_V\beta_3$ expression translated into blood perfusion recovery. A needle-like laser Doppler probe was used to noninvasively determine the degree of blood perfusion in both the ischemic nonischemic limbs of each animal in the immediate pre- and postoperative periods as well as one, two, and three weeks later. We did not find a significant difference between the mMSC- and saline-treated animals one week after femoral artery ligation, however in weeks two and four, blood perfusion increased in the mMSC group by almost 60% relative to the saline group (see Figure 4A).

The next step of our study was to determine if the enhanced angiogenesis and perfusion impacted the muscle function of the diabetic ischemic hindlimb. The study was conducted four weeks after surgery. We found a 1.7-fold increase in muscle strength in the mMSC group relative to the saline group (see Figure 4B).

Finally, to assess organ specific uptake of $^{64}$Cu-NOTA-PEG$_4$-cRGD$_2$ probe *in vivo*, we performed a biodistribution study at 90 minutes after intravascular injection into saline and mMSC treated mice. As expected, the highest uptake was observed in the kidneys due to renal filtration being the dominate excretion route (11.08 ± 0.98, 3.65 ± 0.44 %I.D./g for cortex and medulla, respectively). Relatively high uptake was also observed in the intestines (4.61 ± 0.30), lungs (2.95 ± 0.19), and the spleen (2.24 ± 0.19) (see Figure 3B).

## *In vitro* Post mortem evaluation of mMSCs effect on the ischemic microenviroment of PAD

To investigate the impact of mMSC treatment at the cellular level, at two weeks post transplantation, a subset of animals was euthanized (n=4 for both the mMSC- and saline-treated groups), sections of hindlimb muscle tissue were excised, and stained with a commercially available PE-labeled anti-CD31 (endothelial marker). Subsequent fluorescence imaging showed a 3.3-fold increase in the angiogenic activity of the ischemic stem cell treated hindlimb in comparison to the ischemic saline treated hindlimb (see Figure 5A). Whereas, the non-ischemic saline and non-ischemic stem cell had no significant change in CD31 expression (see Figure 5B-D).

Additional sections of muscle tissue were used to investigate the mRNA expression of several genes involved in the angiogenic process. Globally, we found that gene expression state of the ischemic skeletal muscle of the mMSC-treated group was comparable with that of non-ischemic control muscle, but it differed significantly from the saline treated animals. As expected, samples from the same mouse/array were highly correlated and samples in the same dye had lower levels of correlation. However, after removing the effects of array and dye, principal components analysis clustering showed that the non-ischemic samples from mice administered with saline were not different from non-ischemic samples treated with mMSCs, and there were no

outlier samples (see Figure 6A, B). Moreover, we found almost 2-fold increase in expression of the angiogenic markers HIF1-*a*, $\beta_3$, and $\beta_5$ in the mMSC-treated group relative to the saline-treated group (see Figure 7). We also found that TNF-*a* and CD68 (both markers of inflammation) demonstrated a significant ($p < 0.05$) 1.2-fold enhancement in the saline group, indicating an up-regulation of the inflammatory response. We also noted a 1.2-fold increase in 2,6-phosphofructo-2-kinase, a key enzyme involved in glycolysis, within the mMSC treated tissue.

Sections of ischemic saline- and mMSC-treated muscle tissues were also used to extract and quantify protein expression levels. In accordance with the transcriptomics results, we found an increase in expression of the pro-angiogenic proteins and a decrease in the pro-inflammatory proteins in the stem cell-treated animals relative to the saline-treated animals (see Figure 6C).

## Discussion

Peripheral arterial disease (PAD) involves a broad range of vascular pathologies extending from the cerebral vasculature to lower limb arteries. PAD patients experience insufficient blood flow at rest and during the exercise, which can result in intermittent claudication. Imaging techniques focused on PAD progression have the capability to improve the *status quo* by facilitating earlier detection, guiding patient management decisions, and enabling disease prevention and individualized therapies. The studies presented here utilize novel imaging approaches developed to non-invasively assess the potency of muscle-derived MSCs (mMSCs) as a regenerative therapy to repair and reverse diabetic vascular complications in an established animal model of PAD. A variety of techniques and imaging strategies were applied to quantify angiogenesis, blood flow recovery, muscular function, and gene expression profiles in mMSC-treated ischemic tissue.

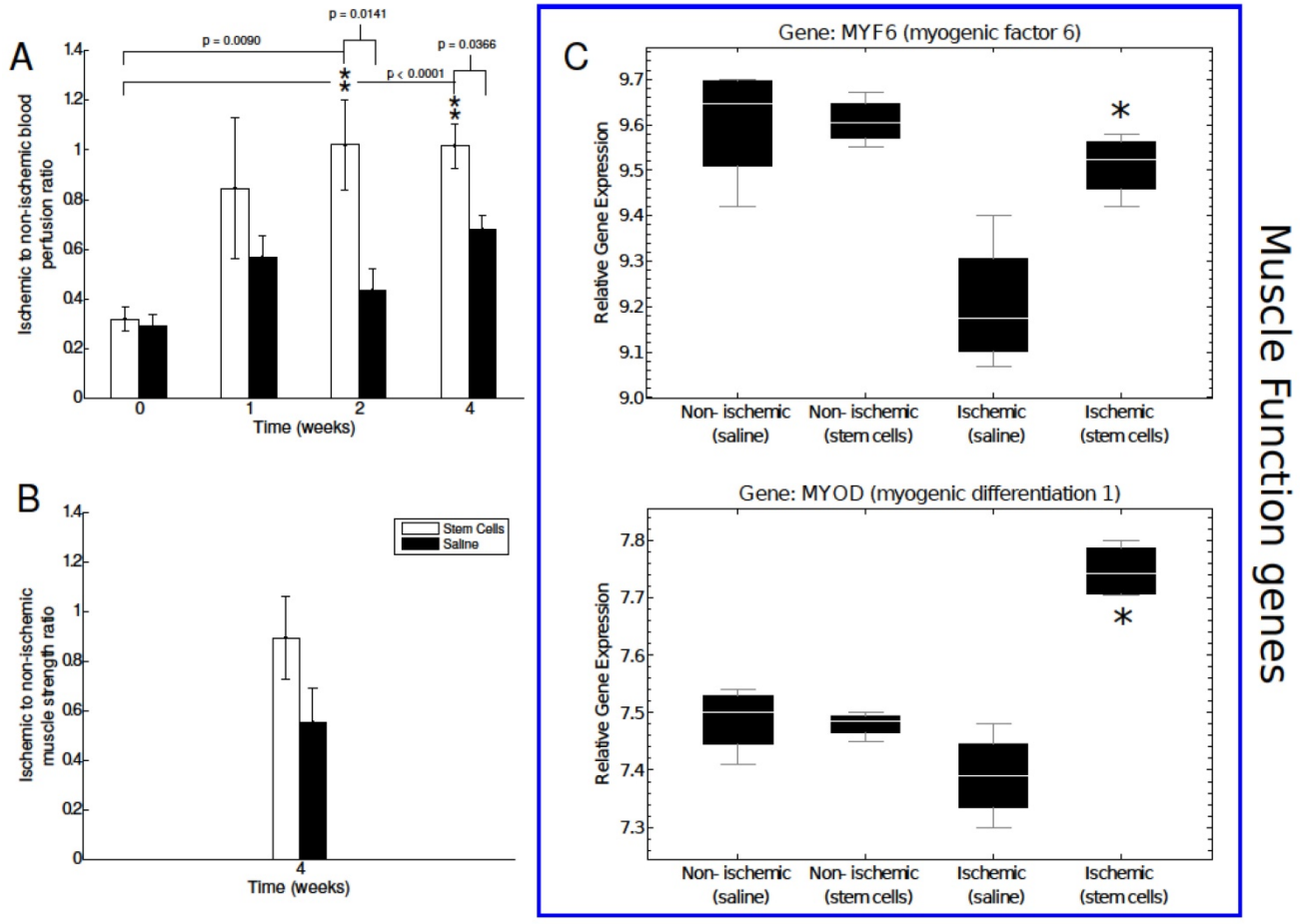


**Figure 4.** Analysis of blood perfusion, muscle strength, and muscle function related gene expression. A) Laser Doppler flow measurements were performed to assess blood perfusion in the ischemic and non-ischemic tissue of our mMSC- and saline-treated mice. Perfusion was significantly enhanced relative to baseline and saline-treated mice at the two and four week time points. B) Muscle function was assessed using an invasive technique at the four-week time point. The mMSC-treated group showed a 1.7-fold increase over the saline-treated mice. C) Key muscle function genes determined by microarray n=4 for each group how a significant up-regulation in ischemic mMSCs treated mice in comparison to the saline and the non-ischemic skeletal muscle. The asterisks indicate a p value of $< 0.01$ comparing ischemic stem cell vs. ischemic saline treated mice.

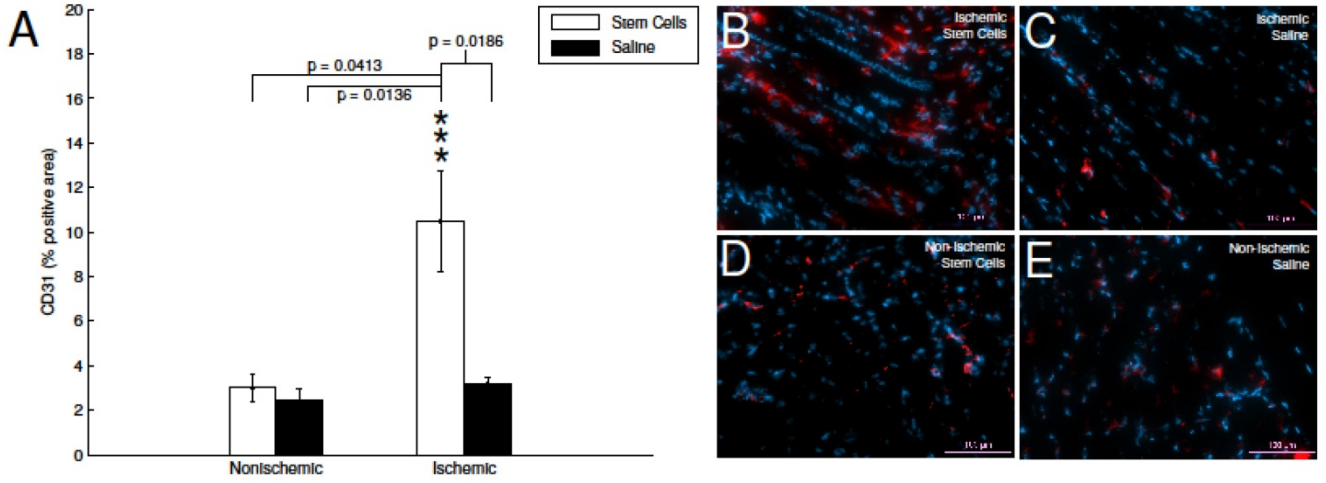


**Figure 5.** CD31immunohistofluorescence. A) Quantification of CD31-positive area in stained skeletal muscle tissue. The mMSC-treated ischemic tissue showed significant enhancement relative to non-ischemic tissue, and saline-treated tissues. B-E) representative immunohistochemistry images with CD31 (red) and DAPI (blue).

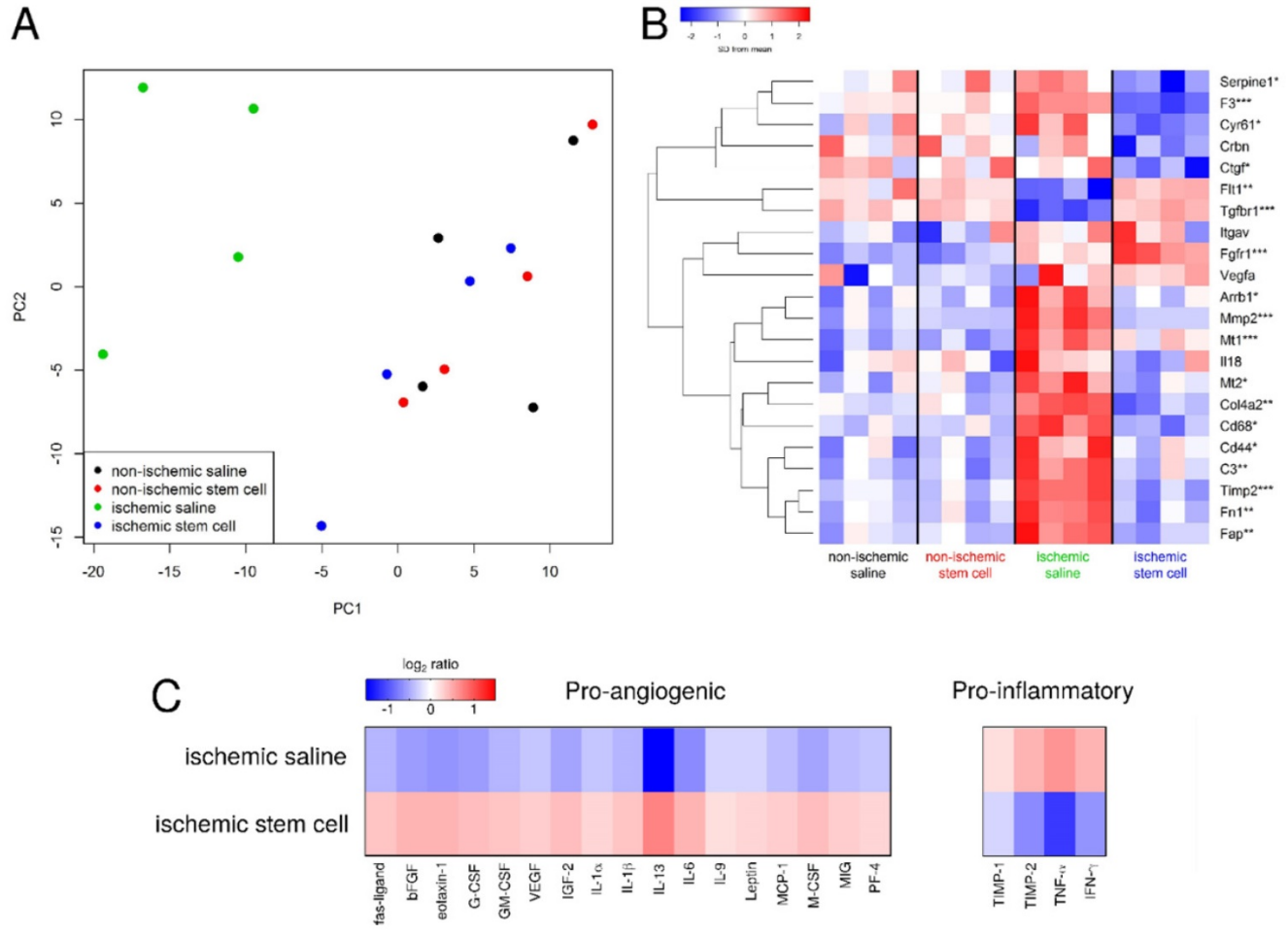


**Figure 6.** Analysis of transcriptomics and proteomics data. A) The gene expression states of excised tissues projected onto the first two principal components. The mMSC-treated ischemic tissue (blue) clusters with the non-ischemic tissues (red and black), indicating similar gene expression profiles, while the saline-treated ischemic samples cluster separately (green). B) Heat map of the expression of several pro- and anti-angiogenic genes in our saline- and mMSC-treated mice (n=4 in each group). Asterisks indicate the smallest FDR p-value across the four comparisons (ischemic saline vs. non-ischemic saline, ischemic stem cell vs. non-ischemic stem cell, ischemic stem cell vs. ischemic saline, overall ANOVA)). * FDR p < 0.2, ** FDR *p* < 0.1, *** FDR *p* < 0.05.C) Heat map of cytokine expression (21 proteins) comparing mMSC- and saline-treated ischemic tissue. For each protein on the cytokine membrane, expression levels for both mMSC- and saline-treated tissues were averaged, and the log2 ratio of each value relative to its respective average is shown.

We began our investigation by non-invasively assessing the expression of $a_V\beta_3$ in our two experimental (mMSC) and control (saline) groups utilizing a cRGD-based PET tracer, $^{64}$Cu-NOTA-$PEG_4$-$cRGD_2$. We observed an increase in the uptake of the probe in the ischemic hindlimb as early as one week after femoral artery ligation and treatment with mMSC. This was confirmed by an ischemic muscle co-stain of CD31 (a key marker for endothelium cell proliferation). Importantly, as mMSCs do not express $a_V\beta_3$ (data not shown), the increased signal we observed was attributable to the physiological effects of the mMSCs' interactions within the ischemic tissue, *to wit* the enhancement of angiogenic activity. Unfortunately, many of the biochemical details of these interactions are complex, poorly understood, and largely beyond the scope of this manuscript. By week four of our study, the enhancement we observed had largely disappeared, indicating either a return to normalcy for the tissue or a diminishment in the therapeutic effect of the mMSCs. Based on the results of our blood perfusion, transcriptomics, and muscle recovery assays (see below), we believe it is more likely the former rather than the later. We next tested the hypothesis that the observed differences in $a_V\beta_3$ expression between mMSC-treated and saline mice would translate into perfusion recovery. We evaluated blood perfusion using a needle-like laser Doppler probe inserted at the gastrocnemius-soleus muscle at one, two, and three weeks after surgery. We saw an increase in perfusion at weeks two and three in mMSC-treated group where there was little or no change in the saline-treated group. This indicates that the enhanced $a_V\beta_3$ activity was indeed associated with neovascularization within the mMSC-treated ischemic tissue. Our results are in agreement with several other published studies that have found that stimulation of angiogenesis promotes the recovery of tissue perfusion [21]. Moreover, these studies investigated the impact of several factors such as age, sex, and genotype, and found an average time of approximately two weeks for perfusion recovery (provided, of course, no essential genes are knocked out)—a timeframe in close agreement with our results.

After establishing non-invasively the therapeutic effects of mMSC transplantation into ischemic limb, we wanted to confirm that the observed changes in peripheral angiogenesis and perfusion were associated with a recovery in muscle function. After the four-week imaging session, an invasive contractile force measurement technique was employed to measure muscle strength in the ischemic and nonischemic hindlimbs of a subset of our animals. We found a 1.7-fold increase in muscle strength in the mMSC-treated group relative to the saline-treated control group. The mean ratio of ischemic to nonischemic muscle strength of mMSCs-treated animals was approximately 0.89, indicating almost full recovery of muscle function. Due to the invasive nature of the measurements, they were performed on only a small subset of animals (n=2 for both the mMSC and saline groups). As such, statistical significance could not be achieved. Instead, we investigated the expression levels of genes in the MyoD family of muscle regulatory factors, which are known to be expressed on satellite cells (located between the basal lamina and sarcolemma of myofibers) and stimulated by damage to the muscle [22]. The mMSC-treated ischemic muscle showed a significant upregulation of the key regulatory genes such as myogenic differentiation 1 (MYOD), and myogenic factor 6 (MYF6) in comparison to the saline-treated ischemic muscle tissue, indicating increased muscle regeneration and healing in mMSC-treated animals (see Figure 4C).

So far, our study has focused on the physiological effects of mMSC treatment at the animal and tissue levels (neovascularization, blood flow recovery, muscle strength). Nevertheless, both PAD and angiogenesis involve a number of cellular-level processes that are orchestrated by a range of microenvironmental cues including those associated with ischemia and hypoxia [23], nitric oxide [24], and inflammation [25]. Investigating how these factors influence the behavior and gene expression state of the cells that make up skeletal muscle tissue, represents an important final part of our study. We performed microarray transcriptomics experiments on excised tissue samples, and attempted to quantify the differential expression of 5 important categories of genes, namely those associated with hypoxia, inflammation, pro-angiogensis, anti-angiogensis, and metabolism (see Figure 7).

Several genes associated with the pro-angiogenic response (such as HIF-1$a$, $\beta_3$ and $\beta_5$, Fgfr1, Tgfbr1, Vegfa, Flt1, and Itgav) were found to be enhanced in mMSC-treated muscles. HIF-1$a$, a transcription factor that mediates the adaptive response to hypoxia and ischemia by promoting angiogenesis, showed a significant increase in mMSC-treated mice compared to the saline group. This confirms that the treatment with mMSCs upregulates the expression of genes involved in initiation of the angiogenic pathway. Interestingly, the ischemic saline treated group actually showed a down-regulation in HIF-1$a$ compared to the nonischemic tissues of our mice. This finding is consistent with other published data, and is attributed to the hyperglycemic environment of the endothelium cells, which is unfavorable for induction of angiogenesis [21].

Expression of these pro-angiogenic genes was found to correlate with metabolic genes such as, fructose-2,6-biphosphatase 2 (Pfkfb2) and the solute carrier family 2 (Slc2a4) genes. It is possible that the vascular remodeling itself may present energy or metabolite requirement, or that the increase in blood flow and subsequent recovery of muscle function associated with vascular repair may lead to increased metabolic activity.

In contrast, we found the expression of several genes associated with inflammation tended to correlate with others known to inhibit angiogenesis. As examples, saline-treated ischemic tissues demonstrated strong upregulation of the pro-inflammatory genes TNF-*a* and CD44 [26, 27] as well as the anti-angiogenic genes interleukin 18 (Il18), arrestin (Arrb1), and the tissue inhibitor of metalloproteinase 2 (Timp2) [28–30] (among others). The mMSC-treated mice showed no such upregulation. These results are in line with a pilot transcriptome study of human patients with type-1 diabetes, in which a clear upregulation of TNF-*a* was observed in functionally impaired endothelial progenitor cells [31]. These results highlight the importance of the tissue microenvironment in establishing the angiogenic response; inflamed tissue inhibits angiogenesis and slows recovery from vascular occlusion.

Additional proteomics studies confirmed the up-regulation of the pro-angiogenic genes and relative down-regulation of the pro-inflammatory genes in our stem cell-treated ischemic tissue.

DM causes changes in the endothelial microenvironment that can make a single biomarker therapy challenging to target PAD. Connective tissue growth factor expression (CTGF, an inhibitor of angiogenesis), cysteine-rich protein 61 (Cyr61), metallothionein 1 (Mt1) and 2 (Mt2), and CD68 (expressed on monocytes/macrophages), as examples, have been shown to be markedly increased in diabetic animals [32] (see Figure 6B). In general, all animals showed enhanced expression of these genes, however the ischemic mMSC-treated tissues displayed a significant down regulation confirming, at the cellular level, the ability of mMSCs to alter the tissue microenvironment in complex ways. Intriguingly, the same set of genes was found to change after acute hindlimb ischemia within healthy mice in as soon as 6 hours and return to homeostasis between 7 to 14 days later, again in accordance with our results [33].

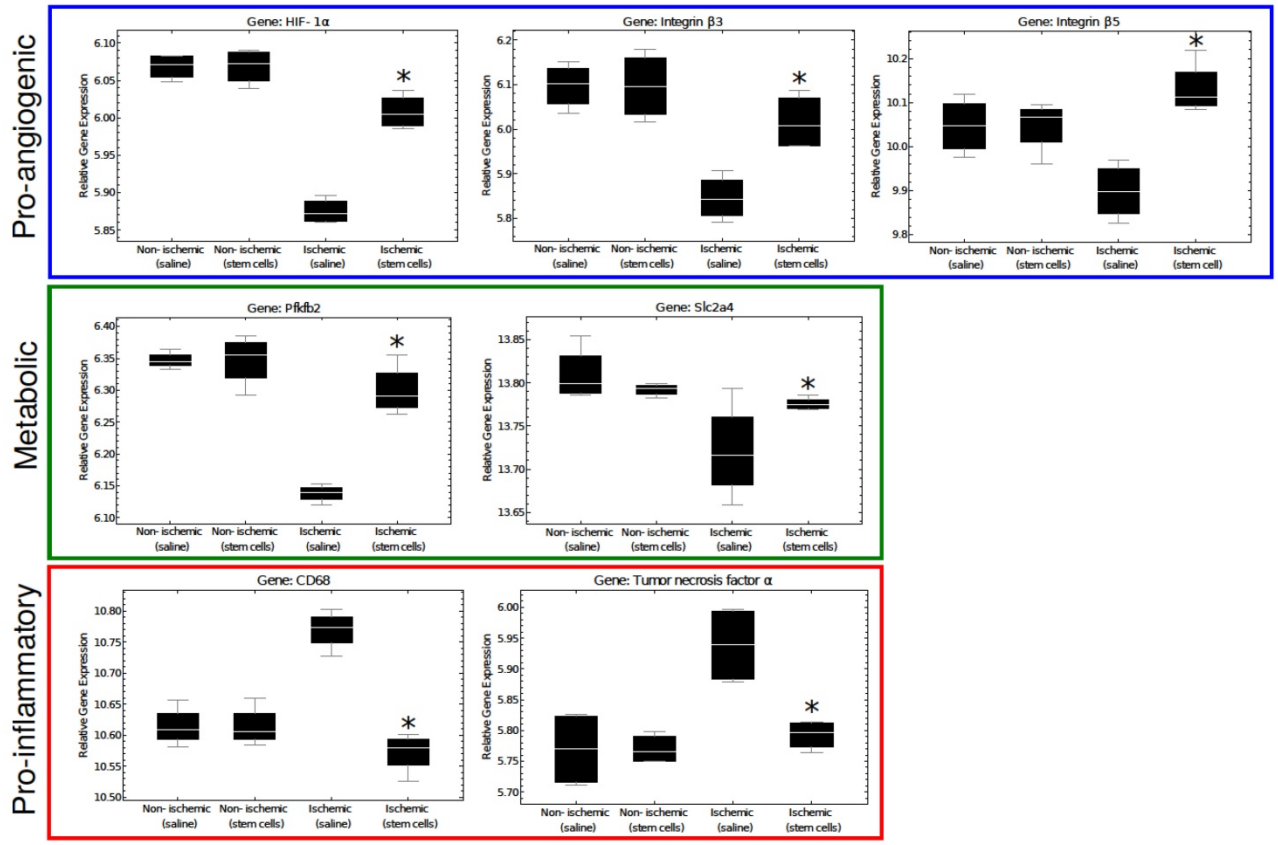


**Figure 7.** A representation of key regulatory genes. Pro-angiogenic and metabolic genes are significantly increased in mMSC-treated ischemic tissue, where pro-inflammatory genes are up-regulated in ischemic saline muscle tissue. There was no difference between the non-ischemic saline vs non-ischemic stem cell treated samples. The asterisks indicate a p value of $< 0.05$ comparing ischemic stem cell vs. ischemic saline treated mice.

Other DM-associated genes that have been shown to increase the risk of thrombosis and vascular disease include Coagulation Factor III (F3) [34], which we found to be significantly ($p = 0.05$) downregulated in our mMSC-treated group (see Figure 6B). Matrix metalloproteinase- 2 (Mmp2), which is implicated in angiogenesis, was upregulated in mMSC group relative to saline animals, however other studies have found no change in its expression [35].

This study pieces together the changes that occur in diabetic mice after femoral artery ligation and therapeutic intervention with mMSCs. All told, our study paints a compelling picture, in which mMSCs exert far-reaching effects, countering the anti-angiogenic effects of DM and inflammation, and enhancing the process of neovascularization and healing. More targeted experiments are needed to elucidate the biochemistry that underpin these responses, but this work represents an important step to widen our knowledge on multifaceted actions of mMSCs in the recovery of vascular complication associated with DM

## Conclusion

Angiogenic tissue microenvironment is tightly controlled by multifactorial processes involving both pro- and anti-angiogenic factors interacting with endothelial cells, smooth muscle cells, and the extracellular matrix (ECM). The signaling pathways are complex, with many details remaining unclear. To date, only a few studies have investigated the effects of diabetes on angiogenesis within the skeletal muscle, and most of them focused almost entirely on a single biomarker (VEGF-A) with ambiguous results [3, 36,37].

Here we present findings that validate the potential for mMSCs to be used as a holistic therapy for diabetes-associated PAD. Rather than targeting a single facet of the body's response to ischemia, mMSCs appear to exert far reaching effects on the ischemic tissue microenvironment by enhancing angiogenesis, decreasing inflammation, and promoting muscle recovery. Our work focuses on the response to treatment at both the cellular and tissue levels. To our knowledge this is the first study to utilize non-invasive targeted imaging strategies to measure angiogenesis and blood flow in ischemic diabetic limbs after muscle-derived mesenchymal stem cells therapy in combination with transcriptomics analysis. The translational nature of this work is difficult to overstate; not only we find that mMSC-based therapy can largely reverse vascular occlusion associated with PAD, but we also provide effective molecular imaging approaches that one day may be used to help diagnose vascular complications, as well as monitor their progression and treatment.

## Acknowledgements

We would like to thank the Roy J. Carver Biotechnology Center at the University of Illinois for their help with the microarray experiment, particularly Dr. Mark Band for the labeling and hybridizations, and Dr. Jenny Drnevich for the statistical analysis. We would also like to thank the Flow Cytometry Facility at Roy J. Carver Biotechnology Center specially Dr. Barbara Pilas for her help with sorting the cells. Finally we thank Dr. Chaitali Misra for her help with the RNA extractions, Dr. Andrzej Czerwinski at Peptides International for his help in the synthesis of $^{64}$Cu-NOTA-PEG$_4$-cRGD$_2$ probe used in this study, Dr. Koyal Garg for her help with muscle function experiments and undergraduate research assistant Than Huynh for help with lab prep and data analysis.

### Funding

Studies were funded by AHA Scientist Development Grant (10SDG4180043, LWD), Arnold Beckman Foundation (JH, ITD, LWD), Diabetes Complications Consortium DiaComp (25732-27, MB, LWD), National Science Foundation Integrative Graduate Education and Research Traineeship (IGERT) in Cellular and Molecular Mechanics and BioNanotechnology (HDH), and National Institute of Biomedical Imaging and Bioengineering of the National Institutes of Health under Award Number T32EB019944 (JH).

## Competing Interests

The authors have declared that no competing interest exists.

## References

[1] Elbert S Huang, Anirban Basu, Michael O'grady, et al. Projecting the future diabetes population size and related costs for the us. Diabetes care. 2009; 32(12): 2225–2229.

[2] [Internet] CDC: Atlanta GA. National diabetes statistics report estimates of diabetes and its burden in the United States, 2014. https://www.cdc.gov/diabetes/pubs/statsreport14/national-diabetes-report-web.pdf.

[3] Alain Rivard, Marcy Silver, Dongfen Chen, et al. Rescue of diabetes-related impairment of angiogenesis by intramuscular gene therapy with adeno-vegf. Am J Pathol. 1999;154(2): 355–363.

[4] Neil P Fam, Subodh Verma, Michael Kutryk, et al. Clinician guide to angiogenesis. Circulation. 2003; 108(21): 2613–2618.

[5] Michael Simons, Robert O Bonow, Nicolas A Chronos, et al. Clinical trials in coronary angiogenesis: issues, problems, consensus. Circulation. 2000; 102(11): e73–e86.

[6] Erica B Sneider, Philip T Nowicki, Louis M Messina. Regenerative medicine in the treatment of peripheral arterial disease. J Cell Biochem. 2009; 108(4): 753–761.

[7] Zankhana Raval, Douglas W Losordo. Cell therapy of peripheral arterial disease. Circ Res. 2013; 112(9): 1288–1302.

[8] Alexandrina Burlacu. Tracking the mesenchymal stem cell fate after transplantation into the infarcted myocardium. Curr Stem Cell Res Ther. 2013; 8(4): 284–291.

[9] Heather D Huntsman, Nicole Zachwieja, Kai Zou, et al. Mesenchymal stem cells con- tribute to vascular growth in skeletal muscle in response to eccentric exercise. Am J Physiol Heart Circ Physiol. 2013; 304(1): H72–H81.
[10] Zoya Tahergorabi, Majid Khazaei. Imbalance of angiogenesis in diabetic complications: the mechanisms. Int J Prev Med. 2012; 3(12).
[11] Lawrence W Dobrucki, Donald P Dione, Leszek Kalinowski, et al. Serial noninvasive targeted imaging of peripheral angiogenesis: validation and application of a semiautomated quantitative approach. J Nucl Med. 2009; 50(8): 1356–1363.
[12] Jamila Hedhli, Andrzej Czerwinski, Matthew Schuelke, et al. Synthesis, chemical characterization and multiscale biological evaluation of a dimeric-cRGD peptide for targeted imaging of α v β 3 integrin activity. Sci Rep. 2017; 7(1): 3185.
[13] Andrew DH Clark, Joanne M Youd, Stephen Rattigan, et al. Heterogeneity of laser doppler flowmetry in perfused muscle indicative of nutritive and nonnutritive flow. Am J Physiol Heart Circ Physiol. 2001; 280(3): H1324–H1333.
[14] Tara N Lueders, Kai Zou, Heather D Huntsman, et al. The α7β1-integrin accelerates fiber hypertrophy and myogenesis following a single bout of eccentric exercise. Am J Physiol Heart Circ Physiol. 2011; 301(4): C938–C946.
[15] J Hua, L W Dobrucki, M M Sadeghi, et al. Noninvasive imaging of angiogenesis with a $^{99m}$Tc-labeled peptide targeted at $a_V\beta_3$ integrin after murine hindlimb ischemia. Circulation. 2005; 111(24): 3255–3260.
[16] Matthew J Denwood. runjags: An r package providing interface utilities, model templates, parallel computing methods and additional distributions for mcmc models in jags. J Stat Softw. 2016; 71(9): 1–25.
[17] Matthew E Ritchie, Belinda Phipson, Di Wu, et al. limma powers differential expression analyses for rna sequencing and microarray studies. Nucleic Acids Res. 2015; : gkv007.
[18] Gordon K Smyth, Terry Speed. Normalization of cDNA microarray data. Methods. 2003; 31(4): 265–273.
[19] Belinda Phipson, Stanley Lee, Ian J Majewski, et al. Robust hyperparameter estimation protects against hypervariable genes and improves power to detect differential expression. Ann Appl Stat. 2016; 10(2): 946–963.
[20] Wolfgang Huber, Vincent J Carey, Robert Gentleman, et al. Orchestrating high-throughput genomic analysis with bioconductor. Nat Methods. 2015; 12(2): 115–121.
[21] Marta Bosch-Marce, Hiroaki Okuyama, Jacob B Wesley, et al. Effects of aging and hypoxia-inducible factor-1 activity on angiogenic cell mobilization and recovery of perfusion after limb ischemia. Circ Res. 2007; 101(12): 1310–1318.
[22] DDW Cornelison, Barbara J Wold. Single-cell analysis of regulatory gene expression in quiescent and activated mouse skeletal muscle satellite cells. Developmental biology. 1997; 191(2): 270–283.
[23] Georges von Degenfeld, Andrea Banfi, Matthew L Springer, et al. Microenvironmental VEGF distribution is critical for stable and functional vessel growth in ischemia. The FASEB journal. 2006; 20(14): 2657–2659.
[24] Mina J Bissell, William C Hines. Why don't we get more cancer? A proposed role of the microenvironment in restraining cancer progression. Nat Med. 2011; 17(3): 320–329.
[25] Nathalie Dehne, Bernhard Brüne. Hif-1 in the inflammatory microenvironment. Exp Cell Res. 2009; 315(11): 1791-1797.
[26] Anita Tandle, Dan G Blazer, Steven K Libutti. Antiangiogenic gene therapy of cancer: recent developments. J Transl Med. 2004; 2(1): 22.
[27] Charlotte Harrison. Obesity and diabetes: Cd44 immune receptor linked to diabetes. Nat Rev Drug Discov. 2012; 11(6): 442–442.
[28] Tai-Ping D Fan, Rhys Jagger, Roy Bicknell. Controlling the vasculature: angiogenesis, anti-angiogenesis and vascular targeting of gene therapy. Trends Pharmacol Sci. 1995; 16(2): 57–66.
[29] ROBERT J D'Amato, Michael S Loughnan, Evelyn Flynn, et al. Thalidomide is an inhibitor of angiogenesis. Proc Natl Acad Sci. 1994; 91(9): 4082–4085.
[30] M Malecki, P Kolsut, R Proczka. Angiogenic and antiangiogenic gene therapy. Gene Ther. 2005; 12: S159–S169.
[31] Olivia van Oostrom, Dominique PV de Kleijn, Joost O Fledderus, et al. Folic acid supplementation normalizes the endothelial progenitor cell transcriptome of patients with type 1 diabetes: a case-control pilot study. Cardiovasc Diabetol. 2009; 8(1): 47.
[32] Riikka Kivel ä̈, Mika Silvennoinen, Anna-Maria Touvra, et al. Effects of experimental type 1 diabetes and exercise training on angiogenic gene expression and cappilarization in skeletal muscle. The FASEB journal. 2006; 20(9): 1570-1572.
[33] Cheol Whan Lee, Eugenio Stabile, Timothy Kinnaird, et al. Temporal patterns of gene expression after acute hindlimb ischemia in mice: insights into the genomic program for collateral vessel development. J Am Coll Cardiol. 2004; 43(3): 474–482.
[34] N Babic□, A Dervisevic□, J Huskic□, et al. Coagulation factor viii activity in diabetic patients. Med Glas. 2011; 8(1): 134-139.
[35] Shiro Uemura, Hidetsugu Matsushita, Wei Li, et al. Diabetes mellitus enhances vascular matrix metalloproteinase activity. Circ Res. 2001; 88(12): 1291–1298.
[36] Ferdinando Carlo Sasso, Daniele Torella, Ornella Carbonara, et al. Increased vascular endothelial growth factor expression but impaired vascular endothelial growth factor receptor signaling in the myocardium of type 2 diabetic patients with chronic coronary heart disease. J Am Coll Cardiol. 2005; 46(5): 827–834.
[37] Eva Chou, Izumi Suzuma, Kerrie J Way, et al. Decreased cardiac expression of vascular endothelial growth factor and its receptors in insulin-resistant and diabetic states. Circulation. 2002; 105(3): 373–379.